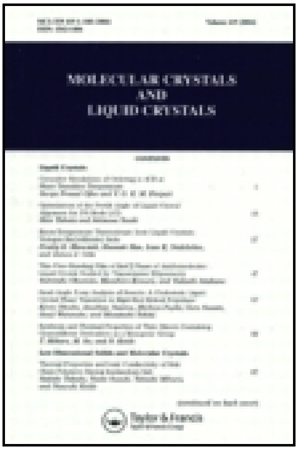

Molecular Crystals and Liquid Crystals
Publication details, including instructions for authors and subscription information:
http://www.tandfonline.com/loi/gmcl16

Microscopic Description of Nematic-Smectic A_2 and Nematic-Smectic A_1-Smectic A_2 Phase Transitions in Binary Mixture of Polar and Nonpolar Liquid Crystals

L. V. Mirantsev [a]

[a] OKB "Register," Institute of Physics, Academy of Sciences of Azerbaijan SSR, Baku, 370143, USSR

Version of record first published: 28 Mar 2007.

To cite this article: L. V. Mirantsev (1987): Microscopic Description of Nematic-Smectic A_2 and Nematic-Smectic A_1-Smectic A_2 Phase Transitions in Binary Mixture of Polar and Nonpolar Liquid Crystals, Molecular Crystals and Liquid Crystals, 142:1-4, 59-76

To link to this article: http://dx.doi.org/10.1080/00268948708084593

Mol. Cryst. Liq. Cryst., 1987, Vol. 142, pp. 59–76
Photocopying permitted by license only

Printed in the United States of America

Microscopic Description of Nematic-Smectic A_2 and Nematic-Smectic A_1-Smectic A_2 Phase Transitions in Binary Mixture of Polar and Nonpolar Liquid Crystals

L. V. MIRANTSEV

OKB "Register," Institute of Physics, Academy of Sciences of Azerbaijan SSR, Baku 370143, USSR

(*Received January 21, 1986*)

In the present paper, in a mean field approximation, we considered binary mixtures of polar and nonpolar liquid crystals (LC) with ideal orientational order. It is assumed that nonpolar molecules can form only monolayer smectic A-structure whereas polar molecules can form both monolayer smectic A-structure with short-range antiferroelectric order and bilayer smectic A-structure with long-range antiferroelectric order. By analogy with McMillan's theory the self-consistent equations determining order parameters for these smectic A structures are introduced. It is shown that smectic A_1 phase with monolayer smectic A structure and smectic A_2 phase with coexisting monolayer and bilayer smectic-A structures can occur in the mixture. Phase diagram for mixture and entropy discontinuities at the nematic-smectic A_1 and smectic A_1-smectic A_2 phase transitions obtained by numerical solution of self-consistent equations are similar to experimental ones. Also the temperature and concentration dependences of intensities of X-ray scattering from monolayer and bilayer smectic A structures are obtained.

Keywords: NSA_1SA_2 phase diagram, X-ray scattering

I. INTRODUCTION

The physical properties of strongly polar liquid crystals (LC) consisting of molecules having end groups (CN or NO_2) with large permanent dipole moment (~4D) are considerably different from those of classical LC.

First, there are smectic A-phases (S_{A_d}) with layer thickness d incommensurate with molecular length l in polar LC and some of such LC demonstrate reentrant phase sequences, nematic (N) → smectic A (S_{A_d}) → reentrant nematic (N_{re})[1-4] and even double reentrant phase sequences N → S_{A_d} → N_{re} → reentrant smectic A phase ($S_{A_{re}}$)[5-8] with decreasing temperature.

Second, the direct transitions between various smectic A-phases take place in some polar LC. For example such transitions are observed in binary mixtures of polar LC 4-pentylphenyl-4-benzoyloxy benzoate (DB5) or 4-hexylphenyl-4-benzoyloxy benzoate (DB6) and nonpolar LC terephtal-bisbutyl aniline (TBBA).[9-11] The bilayer smectic A phase (S_{A_2}) with layer thickness equal to nearly two molecular lengths exists in polar LC DB5 or DB6 and usual monolayer smectic A-phase (S_{A_1}) with layer thickness closed to molecular length occurs in nonpolar LC TBBA. When concentration of nonpolar LC is smaller than certain critical value X_0, then the first order transition N-S_{A_2} is observed with decreasing temperature in such mixtures. In the opposite case, when concentration of nonpolar LC in mixture is larger than X_0, the second order transition N-S_{A_1} takes place first and S_{A_1} phase transits to bilayer S_{A_2} phase with further decreasing temperature.

X-ray studies[10,11] show that only single smectic density wave with period equal to nearly average molecular length l_m in mixture exists in S_{A_1}—phase whereas two density waves with periods closed to l_m and $2l_m$, respectively, coexist in S_{A_2} phase. Thus the S_{A_1}-S_{A_2} transition corresponds to appearance of smectic A structure with period equal (or almost equal) to two average molecular lengths 2 l_m in LC in which smectic A structure with period equal to l_m is already formed.

Also it should be noted that in binary mixtures of two polar LC DB5 and T8 (4-n-octyloxybenzoyloxy-4′-cyanostilbene),[8] the double reentrant phase sequence N-S_{A_d}-N_{re}-$S_{A_{re}}$ as well as several direct transitions between various S_A phases, namely S_{A_d}-S_{A_2}, S_{A_d}-S_{A_1}-S_{A_2} and S_{A_d}-S_{A_1}-$S_{\tilde{A}}$-S_{A_2}, where $S_{\tilde{A}}$ is so-called smectic A antiphase, were observed.

The phenomenological theory of N-S_{A_2} and N-S_{A_1}-S_{A_2} phase transitions was developed by Prost.[12] Microscopic models for S_{A_1} phase and S_{A_2} phase were proposed by de Jeu and Longa.[13] However there are no theoretical papers devoted to detail investigation of N-S_{A_2} and N-S_{A_1}-S_{A_2} transitions and suitable to direct comparison with experimental results.

In the present paper, in a mean field approximation, we considered on the microscopic level S_{A_1} and S_{A_2} phases in binary mixture of polar and nonpolar LC with ideal orientational order. It is assumed that nonpolar molecules can form only monolayer smectic A structure whereas polar molecules can form both monolayer smectic A structure with short-range antiferroelectric order and bilayer smectic A-structure with long-range antiferroelectric order. By analogy with McMillan's theory[14] the smectic order parameters for such smectic A structures are introduced and self-consistent equations determining these parameters are written. As a result of numerical solution of these equations the ranges of stability of N; S_{A_1} and S_{A_2} phases are found and entropy discontinuities at the N-S_{A_2} and S_{A_1}-S_{A_2} transitions are determined. It is shown, that theoretical phase diagram for mixture and concentration dependence of entropy discontinuities are similar to the experimental ones. Also the temperature and concentration dependences of intensities of X-ray scattering from monolayer and bilayer smectic A structures are obtained.

II. MICROSCOPIC DESCRIPTION OF SMECTIC A_1 AND SMECTIC A_2 PHASES IN BINARY MIXTURE OF POLAR AND NONPOLAR LC

Let us consider the liquid crystalline binary mixture of polar (A) and nonpolar (B) molecules. The main difference between these molecules is that polar molecule (A) is asymmetrical and possesses large permanent dipole moment localized at one of molecular ends ("head") and aligned parallel to the long molecular axis, whereas nonpolar molecule (B) is completely symmetrical and not possessing permanent dipole moment. For simplicity let us assume that orientational order in mixture before the transition to smectic A phase is ideal (the long axes of all molecules are oriented parallel to director $\vec{n}$ aligned along Z-axis). This assumption is reasonable enough because the temperatures of experimentally observed N-S_{A_1} and N-S_{A_2} transitions are considerably lower than those of isotropic (I)-N phase transitions.[9-11]

As it was said in the Introduction, the X-rays studies show that both monolayer and bilayer smectic A-structures can take place in pure polar LC whereas only usual monolayer smectic A phase exists in pure nonpolar LC. Therefore it is natural enough to assume that in our mixture the nonpolar and completely symmetrical molecules (B) can form only classical monolayer (with period $d_1 = l_m = (1 - X_B)\, l_A + X_B l_B$, where l_A and l_B are the lengths of polar and nonpolar molecules, respectively, X_B is the concentration of nonpolar molecules in mixture) smectic A structure depicted in Figure 1a.

As for polar molecules (A), since the S_{A_1} and S_{A_2} phases are not ferroelectric the packing of these molecules in such smectic A phases must be antiparallel (i.e. number of molecules with dipoles aligned along director $\vec{n}$ ("up") is equal to that of molecules aligned in opposite direction ("down"). Moreover, dielectric studies[15] of N-S_{A_1} and N-S_{A_2} transitions in pure polar LC DB5 and DB6 as well as in their mixtures with nonpolar LC TBBA revealed the anomalies inherent to the structures with antiferroelectric order. Hence, one can imagine two possible types of antiparallel packing of polar molecules (A) in mixture shown in Figures 1b and 1c, respectively. The first type corresponds to bilayer (with period $d_2 = 2l_m$) smectic A structure with long-range antiferroelectric order because each layer consists of two macroscopic sublayers with mutually opposite alignments of molecular dipoles. The second type of molecular packing corresponds to monolayer (with period $d_1 = l_m$) smectic A structure with short-range antiferroelectric order because each layer consists of coexisting microscopic domains with mutually opposite alignments of molecular dipoles. Hence, monolayer smectic A structure in the mixture formed by the molecules (A) and (B) must be represented as shown in Figure 1d.

Now we have to describe mathematically model packings for monolayer and bilayer smectic A structures. The simplest way for this description is a mean field approximation, in which the effects of short-range order are completely neglected and it is supposed that the state of any molecule depends on only its position in some effective field made by another molecules. In this approximation the equilibrium properties of our mixture are completely described by the following one-particle partition functions for molecules (A) and (B):

$$f_{M=A,B} = Z_M^{-1}\,\delta(\cos^2\theta_M - 1)\exp[-V_T^{(M)}(Z_M)/K_BT], \qquad (1)$$

where $V_T^{(M)}(Z_M)$ is the one-particle pseudopotential defining translational ordering along Z axis of geometric centres of molecules (M) in LC (i.e. layer structure) in smectic A phase, Z_M is the coordinate of the geometric centre of molecule (M), θ_M is the polar angle between long molecule axis and director $\vec{n}$, $\delta(x)$ is the Dirac delta function, defining ideal orientational order in LC, T is the absolute temperature of mixture, K_B is the Boltzmann constant and Z_M is the normalization constant.

By analogy with McMillan's theory[14] the pseudopotentials $V_T^{(A)}$ (Z_A) and $V_T^{(B)}$ (Z_B) defining the monolayer with short-range antiferroelectric order and the bilayer with long-range antiferroelectric order

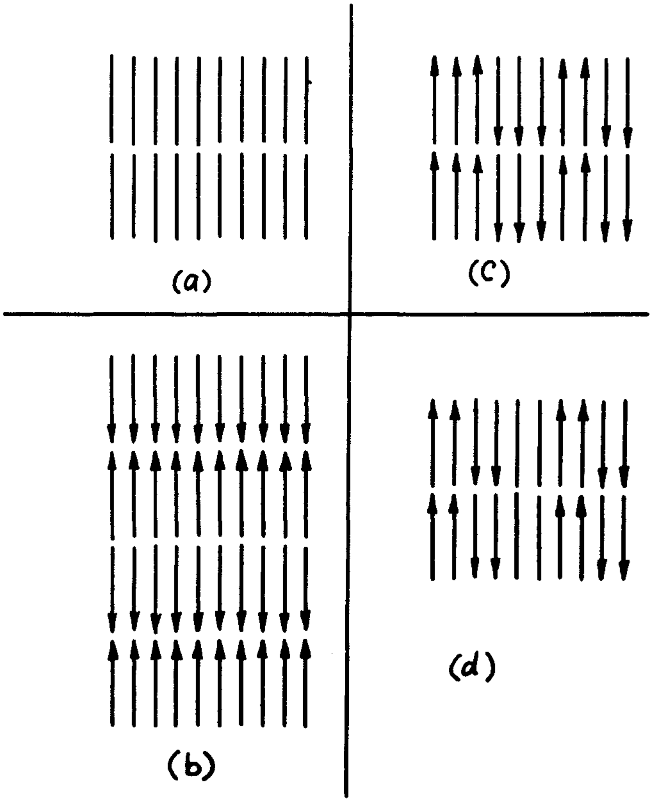

FIGURE 1. a) The classical monolayer smectic A structure formed by the nonpolar molecules (B); b) Bilayer smectic A structure with long-range antiferroelectric order formed by the polar molecules (A). The arrows indicate the molecular dipole directions; c) Monolayer smectic A structure with short-range antiferroelectric order formed by the polar molecules (A); d) Monolayer smectic A structure in the mixture of polar and nonpolar molecules.

smectic A packings of polar molecules (A) and classical monolayer smectic A packing of nonpolar molecules (B), respectively, can be chosen as

$$V_T^{(A)}(Z_A) = -\left[V_{AA}^{(1)}(1 - X_B)\sigma_A^{(1)} + V_{AB}^{(1)} X_B \sigma_B^{(1)}\right]$$

$$\cos(2\pi Z_A/l_m) - \bar{\bar{\bar{S}}} V_{AA}^{(2)}(1 - X_B)\sigma_A^{(2)}\cos(2\pi Z_A/2l_m), \qquad (2)$$

$$V_T^{(B)}(Z_B) = -\left[V_{AB}^{(1)}(1 - X_B)\sigma_A^{(1)} + V_{BB}^{(1)} X_B \sigma_B^{(1)}\right]\cos(2\pi Z_B/l_m), \qquad (3)$$

where $\sigma^{(1)}_{\mathrm{A,B}}$ are the smectic order parameters for molecules (A) and molecules (B), defining monolayer smectic A ordering of these molecules in mixture, $\sigma^{(2)}_{\mathrm{A}}$ is the smectic order parameter defining bilayer smectic A ordering of molecules (A), $V^{(1)}_{AA}$, $V^{(2)}_{AA}$, $V^{(1)}_{AB}$, $V^{(1)}_{BB}$ are the constants defining interaction strength of molecules (A) with each other, molecules (A) with molecules (B), and molecules (B) with each other, respectively, $\overline{\overline{S}}$ is the variable equal to $+1$ for the polar molecules (A) with dipole moment aligned parallel to director n ("up") and -1 for the polar molecules (A) aligned in opposite direction ("down").

Also by analogy with McMillan's theory[14] let us define the smectic order parameters $\sigma^{(1)}_{A,B}$ and $\sigma^{(2)}_{A}$ by the following self-consistent equations:

$$\sigma^{(1)}_{A} = (1/2) \sum_{S=+1,-1} \langle \cos(2\pi Z_A/l_m) \rangle_S$$

$$= (1/2) \sum_{S=+1,-1} \int dZ_A d(\cos\theta_A) \cos(2\pi Z_A/l_m) f_{AS} / \int dZ_A d(\cos\theta_A) f_{AS}, \tag{4}$$

$$\begin{aligned} \sigma^{(1)}_{B} &= \langle \cos(2\pi Z_B/l_m) \rangle \\ &= \int dZ_B d(\cos\theta_B) \cos(2\pi Z_B/l_m) f_B / \int dZ_B d(\cos\theta_B)\, f_B, \end{aligned} \tag{5}$$

$$\begin{aligned} \overline{\overline{S}}\sigma^{(2)}_{A} &= \langle \cos(2\pi Z_A/2l_m) \rangle_S \\ &= \int dZ_A d(\cos\theta_A) \cos(2\pi Z_A/2l_m) f_{AS} / \int dZ_A d(\cos\theta_A)\, f_{AS}, \end{aligned} \tag{6}$$

where (4) is averaged on the alignments of dipoles of molecules (A) because the monolayer smectic A ordering of polar molecules is independent of the dipole alignment.

The free F and internal U energies and the entropy $\underline{\underline{S}}$ of our mixture are given by

$$F = F_N + U - U_N - T(\underline{\underline{S}} - \underline{\underline{S}}_N), \tag{7}$$

$$U - U_N = -(N/2)\left[(1/2) \sum_{S=+1,-1} (1 - X_B) \langle V^{(\mathrm{A})}_{\mathrm{T}} \rangle_S + X_B \langle V^{(B)}_{T} \rangle \right]$$

$$= -(N/2)[(1 - X_B)^2 (V^{(1)}_{AA} \sigma^{(1)^2}_{A} + V^{(2)}_{AA} \sigma^{(2)^2}_{A})$$

$$+ 2X_B(1 - X_B)\, V^{(1)}_{AB} \sigma^{(1)}_{A} \sigma^{(1)}_{B} + X^2_B V^{(1)}_{BB} \sigma^{(1)^2}_{B}], \tag{8}$$

$$-T(\underline{\underline{S}} - \underline{\underline{S}}_N) = -2(U - U_N) - NK_BT\{(1 - X_B)\ln((2l_m)^{-1}\int \mathrm{f}_{AS}\mathrm{d}Z_A\mathrm{d}(\cos\theta_A)) + + X_B\ln(\mathrm{l}_m^{-1}\int f_B dZ_B d(\cos\theta_B))\}, \quad (9)$$

where N is the total number of molecules in mixture, $F_N(U_N)$ and S_N are the free (internal) energy and the entropy of the mixture in nematic phase, respectively.

If the interaction constants $V_{AA}^{(1)}$, $V_{AA}^{(2)}$, $V_{AB}^{(1)}$ and $V_{BB}^{(1)}$ are assumed to be related by $V_{AB}^{(1)}/V_{AA}^{(1)} = V_{BB}^{(1)}/V_{AB}^{(1)} = \beta$, $V_{AA}^{(1)}/V_{AA}^{(2)} = \alpha$ then the pseudopotentials (2) and (3) and one particle partition functions (1) are dependent on only two new effective parameters

$$\sigma_1 = (1/t)[(1 - X_B)\sigma_A^{(1)} + \beta X_B\sigma_B^{(1)}]$$

and $\sigma_2 = (1/t)(1 - X_B)\sigma_A^{(2)}$, where $t = K_BT/V_{AA}^{(2)}$ is the reduced temperature of mixture and equations (4)—(6) can be reduced to the following pair of self-consistent equations

$$\sigma_1 = (1/t)[(1 - X_B)(I_3/I_1) + \beta X_B(I_4/I_2)], \quad (10)$$

$$\sigma_2 = (1/t)(1 - X_B)(I_5/I_1), \quad (11)$$

and the free energy F of mixture is given by

$$F = F_N + NK_BT\{(t/2)(\alpha\sigma_1^2 + \sigma_2^2) - (1 - X_B)\ln I_1 - X_B\ln I_2\}, \quad (12)$$

where

$$I_1 = (2l_m)^{-1}\int_0^{2l_m} dZ_A\exp\{\sigma_2\cos(2\pi Z_A/2l_m) + \alpha\sigma_1\cos(2\pi Z_A/l_m)\}, \quad (13)$$

$$I_2 = l_m^{-1}\int_0^{l_m} dZ_B\exp\{\alpha\beta\sigma_1\cos(2\pi Z_B/l_m)\}, \quad (14)$$

$$I_3 = (2l_m)^{-1}\int_0^{2l_m} dZ_A\cos(2\pi Z_A/l_m)\exp\{\sigma_2\cos(2\pi Z_A/2l_m) + \alpha\sigma_1\cos(2\pi Z_A/l_m)\}, \quad (15)$$

$$I_4 = l_m^{-1}\int_0^{l_m} dZ_B \cos(2\pi Z_B/l_m)\exp\{\alpha\beta\sigma_1\cos(2\pi Z_B/l_m)\}, \tag{16}$$

$$I_5 = (2l_m)^{-1}\int_0^{2l_m} dZ_A \cos(2\pi Z_A/2l_m)\exp\{\sigma_2\cos(2\pi Z_A/2l_m) + \alpha\sigma_1\cos(2\pi Z_A/l_m)\} \tag{17}$$

The results of numerical solution of equations (10) and (11) are presented in Sec. 3. Now one can show that our model contains the phenomenological Prost's model[12] as a some approximation. If in (12) $\ln I_1$ and $\ln I_2$ are expanded in a series of σ_1 and σ_2 parameters then the free energy F is given by

$$F = F_N + NK_BT\{A_1\sigma_1^2 + A_2\sigma_2^2 - D\sigma_2^2\sigma_1 + C_1\sigma_1^4 + C_2\sigma_2^4 + \ldots\}, \tag{18}$$

where

$$\begin{aligned} A_1 &= (\alpha/4)(2t - \alpha[1 + (\beta^2 - 1)X_B]),\\ A_2 &= (2t - (1 - X_B))/4,\\ D &= \alpha(1 - X_B)/8,\\ C_1 &= \alpha^4[1 + (\beta^4 - 1)X_B]/64,\\ C_2 &= (1 - X_B)/64 \end{aligned} \tag{19}$$

Expression (18) is completely analogous to free energy introduced phenomenologically by Meyer and Lubensky[16] and applied by Prost[12] to description of the $N - S_{A_2}$ and $N - S_{A_1} - S_{A_2}$ phase transitions. Minimizing (18) one can obtain the pair of algebraic equations

$$\partial F/\partial\sigma_1 = 2A_1\sigma_1 - D\sigma_2^2 + 4C_1\sigma_1^3 = 0, \tag{20}$$

$$\partial F/\partial\sigma_2 = 2A_2\sigma_2 - 2D\sigma_2\sigma_1 + 4C_2\sigma_2^3 = 0 \tag{21}$$

It is easily seen that the following solutions of equations (20), (21) are possible (in principle): $\sigma_1 = \sigma_2 = 0$ (N phase); $\sigma_1 \neq 0$, $\sigma_2 = 0$

(S_{A_1} phase); $\sigma_1 \neq 0$, $\sigma_2 \neq 0$ (S_{A_2} phase). The solution $\sigma_1 = 0$, $\sigma_2 \neq 0$ is impossible because it does not satisfy Eq. (20). Thus, pure monolayer S_{A_1} phase and coexisting monolayer and bilayer smectic A structures (S_{A_2}) can take place in our mixture. Pure bilayer smectic A structure can not exist without monolayer one. Also it is seen from expansion (18) that the N-S_{A_1} transition (at $\sigma_2 = 0$) always is the second order transition whereas both the N-S_{A_2} and S_{A_1}-S_{A_2} transitions can be the first order as well as second order transitions.

It should be noted that expansion (18) allows to reveal only the general features of possible smectic A phases in mixture. This expansion is too rough and can not be applied to calculations of phase diagram and characteristics of N-S_{A_2} and NS_{A_1}-S_{A_2} transitions suitable to the comparison with experimental results.

III. THE NUMERICAL SOLUTION OF SELF-CONSISTENT EQUATIONS. PHASE DIAGRAM FOR MIXTURE AND THE ENTROPY DISCONTINUITIES AT THE N-S_{A_2} AND S_{A_1}-S_{A_2} TRANSITIONS. COMPARISON WITH EXPERIMENTAL RESULTS

The self-consistent equations (10), (11) were solved numerically in a way similar to one used in Ref. 14 and the solution minimizing the free energy of mixture at the given concentration X_B and reduced temperature t was selected from all possible solutions corresponding to N phase ($\sigma_1 = \sigma_2 = 0$), S_{A_1} phase ($\sigma_1^1 \neq 0$, $\sigma_2 = 0$) and S_{A_2} phase ($\sigma_1 \neq 0$, $\sigma_2 \neq 0$). At the N-S_{A_2} transition points $F_{S_{A_2}} = F_N$ and at the S_{A_1}-S_{A_2} ones $F_{S_{A_2}} = F_{S_{A_1}}$. The N-SA_1 second order transition line can be obtained from the condition $A_1(X_B,t) = 0$. The entropy discontinuities at the N-S_{A_2} and S_{A_1}-S_{A_2} transitions are given by

$$\Delta \underline{\underline{S}}_{N-S_{A2}} = (1/2)NK_Bt\,(\sigma_2^2 + \alpha\sigma_1^2), \tag{22}$$

$$\Delta \underline{\underline{S}}_{S_{A1}-S_{A2}} = (1/2)NK_Bt[\sigma_2^2 + \alpha(\sigma_1^2 - \sigma_1^{1^2})] \tag{23}$$

The phase diagram obtained by the numerical solution of equations (10) and (11) and theoretical expressions (21) and (22) for the entropy discontinuities were compared with Ref. 9 because the most detailed results of calorimetric investigaties of N-S_{A_2} and N-S_{A_1}-S_{A_2} transitions in the DB5-TBBA mixture are brought in this paper. In the first place we had to choose the values for two model parameters α and β. It is seen from (19) that the reduced temperature t_{X_B} of the N-S_{A_1} second order transition in our mixture is a linear function of the concentration X_B and the model parameter β can be determined as $\beta = [(t_{X_B}/t_0 - 1)X_B^{-1}]^{1/2}$, where t_0 is the reduced temperature of this transition extrapolated to $X_B = 0$. It is clearly seen from Figure 2 that the experimental N-S_{A_1} transition line is really the straight one corresponding to value $\beta = 1.2$ which was used in our computations. It is also shown in Figure 2 that experimental N-S_{A_2} transition line for the DB5-TBBA mixture turns into the S_{A_1}-S_{A_2} transition line after crossing with N-S_{A_1} one at the TBBA concentration $X_B = 0.12$. Therefore the α parameter was being varied (at the fixed $\beta = 1.2$) till the theoretical phase diagram with the N$S_{A_1}S_{A_2}$ triple point at $X_B = 0.12$ was obtained. This phase diagram computed at $\alpha = 0.9$ is depicted in Figure 2.

It is seen that though computed absolute temperatures of the N-S_{A_2}, N-S_{A_1} and S_{A_1}-S_{A_2} transitions in mixture normalized to ab-

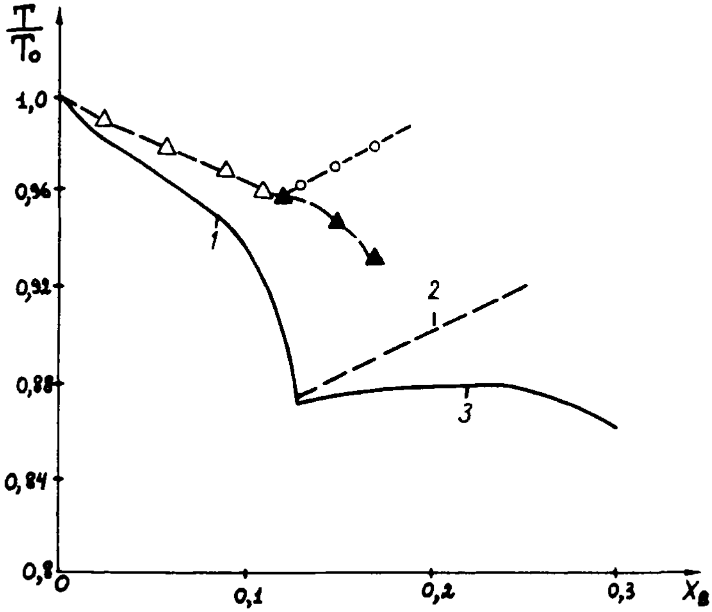

FIGURE 2. The theoretical and experimental phase diagrams for the mixture of the polar and nonpolar LC. To is the absolute temperature of the N-S_{A_2} phase transition in the pure polar LC. 1—The theoretical N-S_{A_2} transition line; 2—the theoretical N-S_{A_1} transition line; 3—the theoretical S_{A_1}-S_{A_2} transition line; —△—the experimental N-S_{A_2} transition points;—○—the experimental N-S_{A_1} transition points;—▲—the experimental S_{A_1}-S_{A_2} transition points.

solute temperature of N-S_{A_2} transition in the pure polar LC are lower than experimental ones the difference between them does not exceed 10%. In general the theoretical phase diagram is very similar to the experimental one.

The computed concentration dependence of the entropy discontinuities at the N-S_{A_2} and S_{A_1}-S_{A_2} transitions in mixture normalized to the entropy discontinuity at the N-S_{A_2} transition in pure polar LC and the corresponding experimental points[9] are shown in Figure 3. It is seen that theory is in well enough agreement with experiment. However, the theoretical absolute values of entropy discontinuities are about 1.6 times larger than the experimental ones. Probably the mean field approximation always gives the excessive entropy discontinuities at the phase transitions[14] because of the mixing of pretransitional, transitional and after transitional changes in the system.

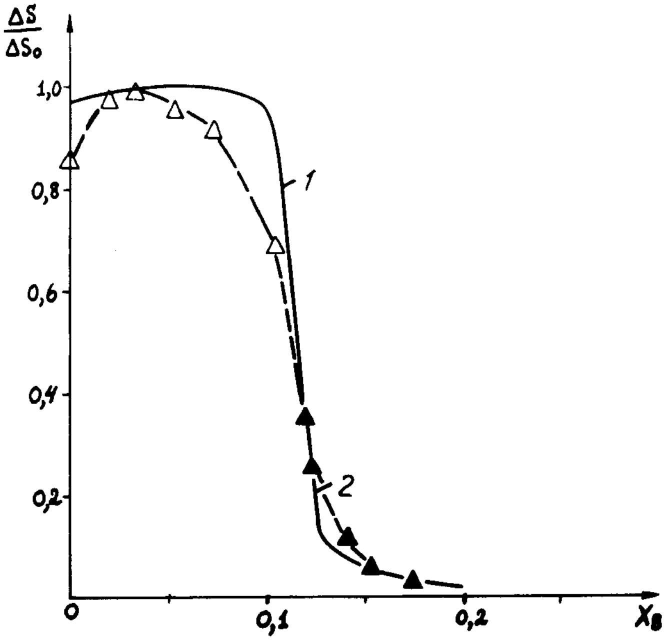

FIGURE 3. The concentration dependence of the entropy discontinuities at the N-S_{A_2} and S_{A_1}-S_{A_2} phase transitions. $\underline{S}_0$ is the entropy discontinuity at the N-S_{A_2} phase transition in the pure polar LC. 1—the theoretical dependence of the entropy discontinuity at the N-S_{A_2} transition; 2—the same dependence for the S_{A_1}-S_{A_2} transition; △—the experimental points of the N-S_{A_2} transition; ▲—the experimental points of the S_{A_1}- S_{A_2} transition.

IV. THE INTENSITIES OF X-RAY SCATTERING FROM MONOLAYER AND BILAYER SMECTIC A STRUCTURES

The X-ray studies give us the most direct information about the smectic A ordering in LC. In particular the smectic order parameter can be determined by the measurement of intensity of X-ray scattering from smectic layers.[17] Therefore it should be useful to obtain in framework of our model the temperature and concentration dependences of intensities of X-ray scattering from the monolayer and bilayer smectic A structures.

Let us consider the situation (corresponding to the experimental one)[10,11] when our LC mixture is perfectly aligned along Z axis and the initial (monochromatic and nonpolarized) X-ray beam is perpendicular to the alignment direction. According to the general X-ray scattering theory[18] the cross-section $d\sigma$ defined as a ratio of intensity scattered into the solid angle $d\Omega$ to the intensity of initial beam is given by

$$d\sigma = (1/2)(e^2/mc^2)^2\,(1 + \cos^2\theta)\left|\int n(\vec{r})e^{-i\vec{q}\vec{r}}d^3\vec{r}\right|^2 d\Omega, \tag{24}$$

where θ is the angle between the wave vectors $\vec{K}$ and $\vec{K}'$ ($|\vec{K}| = |\vec{K}'|$) of initial and scattered beams, respectively, $\vec{q} = \vec{K}' - \vec{K}$, $n(\vec{r})$ is the electron density and (e^2/mc^2) is the classical electron radius.

Since in our LC mixture the molecules can form both monolayer and bilayer smectic A structures with the periods equal to l_m and 2 l_m, respectively, the electron density in the mixture is the periodic in Z and can be expanded in the Fourier series as follows

$$n(z) = \sum_{K=0}^{\infty} b_K e^{iK(2\pi/2l_m)Z}, \tag{25}$$

$$b_K = (2l_m)^{-1}\int_0^{2l_m} n(z)e^{-iK(2\pi/2l_m)Z}\,dZ \tag{26}$$

Then the scattered radiation consists of the set of diffraction maxima and the K^{th} order maximum intensity is proportional to[18]

$$(1 + \cos^2\theta_K)|b_K|^2, \tag{27}$$

where scattering angle θ_k is given by

$$2|\vec{K}| \sin(\theta_K/2) = K(2\pi/2l_m) \tag{28}$$

Since we are interested in only first order ($k = 1$) and second order ($k = 2$) diffraction maxima corresponding to scattering from the bilayer and monolayer smectic A structures, respectively, it is necessary to determine coefficients $|b_1|^2$ and $|b_2|^2$.

Let us express the electron density in the plane, parallel to (x, y) one and crossing Z axis at the Z point in terms of the one particle partition functions (1) for the polar (A) and nonpolar (B) molecules. In the first place we have to remember that the LC molecules consist of the several tens of atoms and each of atoms contains the several electrons. In addition, the distances between atoms (or the atomic groups) in these molecules are comparable with the X-ray wave length λ ($\lambda_{\mathrm{CuK}_\alpha} = 1.54$ Å).[11] Therefore we have to take into account the electron distributions inside the LC molecules. Because of the ideal orientational order in our mixture one can restrict to the electron distribution along the long molecular axis.

At first let us consider the nonpolar molecules (B). The contribution of electrons contained inside the nonpolar molecules within interval from L to $L + dL$, where L is the distance to the molecular geometric center along the long axis (L can vary from $-l_B/2$ to $+l_B/2$), to the electron density at Z point is equal to

$$n_0 X_B n_B(L) f_B(Z - L) dL,$$

where $n_B(L)$ is the linear electron density along the long molecular axis in the nonpolar molecule (B) and n_0 is the total molecular density in mixture. Then the total contribution of all electrons of nonpolar molecules (B) to the electron density $n(Z)$ is equal to

$$n_0 X_B \int_{-l_B/2}^{+l_B/2} n_B(L) f_B(Z - L)\, dL$$

Considering in similar manner the polar molecules (A) one can show that the total contribution of all their electrons to the electron density $n(Z)$ is equal to

$$(1/2) n_0 (1 - X_B) \sum_{S=+1,-1} \int_{-l_A/2}^{+l_A/2} n_A(L) f_{AS}(Z - \bar{S}L)\, dL,$$

where $n_A(L)$ is the linear electron density along the long molecular axis in the polar molecule (A). Thus we obtain the following expression for the electron density in our LC mixture

$$n(Z) = n_0\left\{X_B \int_{-l_B/2}^{+l_B/2} n_B(L)\, f_B(Z - L)dL + (1/2)(1 - X_B) \right. \tag{29}$$
$$\left. \times \sum_{S=+1,-1} \int_{-l_A/2}^{+l_A/2} n_A(L)\, f_{AS}(Z - \bar{\bar{S}}L)\, dL\right\},$$

Inserting (29) into (26) and taking into account Equations (4)–(6) one can obtain

$$|b_1|^2 \sim (1 - X_B)^2 A^2 \sigma_A^{(2)2}, \tag{30}$$

$$|b_2|^2 \sim [(1 - X_B)\, B\sigma_A^{(1)} + X_B C\sigma_B^{(1)}]^2, \tag{31}$$

where

$$A = \int_{-l_A/2}^{+l_A/2} n_A(L) \sin(\pi L/l_m)\, dL, \tag{32}$$

$$B = \int_{-l_A/2}^{+l_A/2} n_A(L) \cos(2\pi L/l_m)\, dL, \tag{33}$$

$$C = \int_{-l_B/2}^{+l_B/2} n_B(L) \cos(2\pi L/l_m)\, dL, \tag{34}$$

and the order parameters $\sigma_{A,B}^{(1)}$ and $\sigma_A^{(2)}$ can be obtained from the solution of selfconsistent Equations (10) and (11).

In order to simplify the computations the atoms (or atomic groups) contained inside the polar and nonpolar molecules are assumed to be the point like. Then the linear electron density along the long molecular axis may be represented as

$$n_{A,B}(L) = \sum_i N_{A,B}(L_i)\delta(L - L_i), \tag{35}$$

and the integrals (32)–(34) are reduced to the following sums

$$A = \sum_{+l_A/2 \geqslant L_i \geqslant -l_A/2} N_A(L_i) \sin(\pi L_i/l_m), \tag{36}$$

$$B = \sum_{+l_A/2 \geq L_i \geq -l_A/2} N_A(L_i) \cos\,(2\pi L_i/l_m), \tag{37}$$

$$C = \sum_{+l_B/2 \geq L_i \geq -l_B/2} N_B(L_i) \cos(2\pi L_i/l_m), \tag{38}$$

where Li is the distance from the i^{th} atom (or i^{th} atomic group) to the molecular geometric center along the long axis and $N_{A,B}(L_i)$ is the number of electrons belonging to this atom (atomic group).

Since the numerical solution of self-consistent equations (10) and (11) was fitted to the results of Ref. 9 in which the DB5-TBBA LC mixture was studied the sums (36)–(38) were computed just for DB5 and TBBA molecules.

The temperature dependences of the first order and second order diffraction maxima intensities calculated through formulae (27), (28), (30) and (31) with order parameters $\sigma^{(1)}_{A,B}$ and $\sigma^{(2)}_{A}$ determined from the solution of self-consistent equations (10) and (11) at the chosen in Sec. 3 values of model parameters α and β are shown in Figure 4.

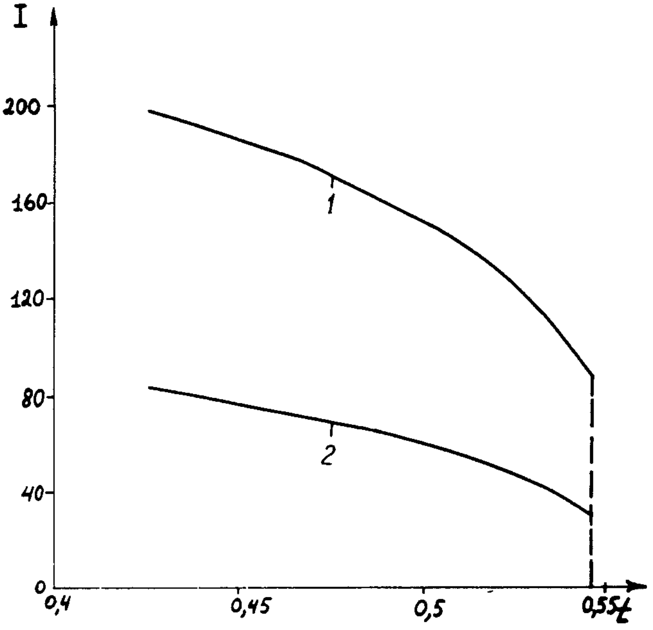

FIGURE 4. The temperature dependences of the first order and second order X-ray diffraction maxima intensities for (in arbitrary units) the pure polar LC. 1—the first order diffraction maximum; 2—the second order diffraction maximum.

It is seen that both maxima appear sharply and simultaneously and then their intensities smoothly increase with decreasing temperature that corresponds to the N-S_{A_2} first order transition and subsequent development of the S_{A_2} phase. It should be noted that the first order diffraction maximum intensity is not more than 3 times larger than second order diffraction maximum one, that is in qualitative agreement with results of X-ray studies because in Ref. 10 it was emphasized that both diffraction maxima intensities are of the same order.

When the nonpolar LC (B) is added to the polar LC (A) (but $X_B < 0{,}12$) the first order diffraction maximum intensity decreases and the second order diffraction maximum one increases (see the Figure 5). Finally, when the nonpolar LC concentration exceeds the critical value ($X_B > 0{,}12$) then the second order diffraction maximum smoothly appears at first and the first order one is adding to it with further decreasing temperature (see Figure 6) that corresponds to the second order transition from N phase to S_{A_1} phase and the subsequent transition from S_{A_1} phase to S_{A_2} phase. It should be added that in S_{A_2}

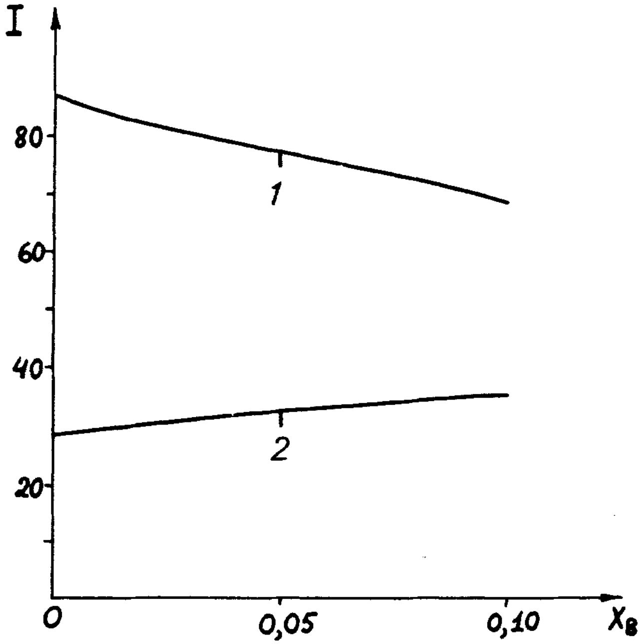

FIGURE 5. The concentration dependences of the first order and second order X-ray diffraction maxima intensities at the N-S_{A_2} transition. 1—the first order diffraction maximum; 2—the second order diffraction maximum.

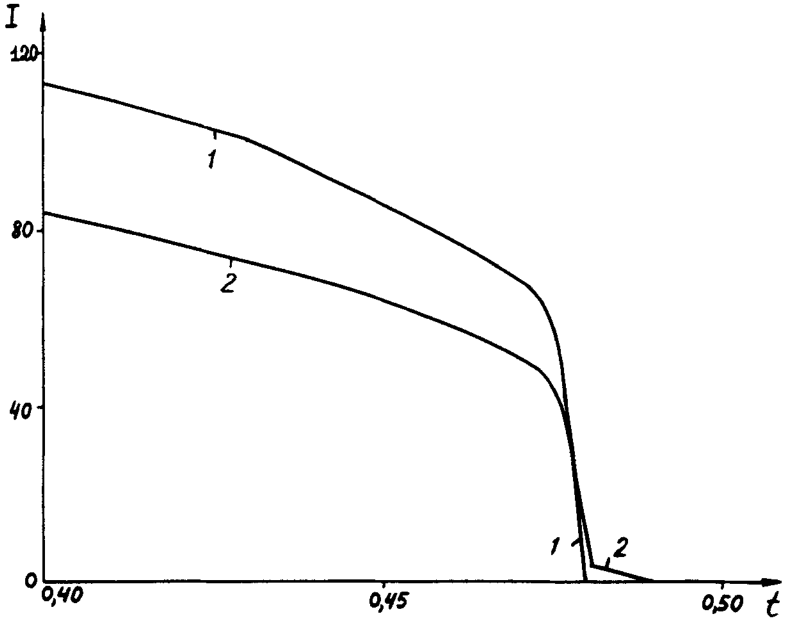

FIGURE 6. The temperature dependences of the first order and second order X-ray diffraction maxima intensities for the 20% mixture (X_B = 0,2) of polar and non-polar molecules. 1—the first order diffraction maximum; 2—the second order diffraction maximum.

phase the second order diffraction maximum intensity is larger than one in S_{A_1} phase that is also in qualitative agreement with experimentally observed picture.[10]

References

1. Cladis, P. E., *Phys. Rev. Lett.*, **35**, 48 (1975).
2. Cladis, P. E., Bogardus, R. K. and Aadsen D., *Phys. Rev.*, **A18**, 2292 (1978).
3. Leadbetter, A. J., Frost, J. C. et al., *J. Phys.*, **40**, 375 (1979).
4. Vani, G. V., *Mol. Cryst. Liq. Cryst.*, **98**, 275 (1983).
5. Hardouin, F., Sigaud, G. et al., *Phys. Lett.*, **71A**, 347 (1979).
6. Hardouin, F., Sigaud, G. et al., *Solid State Commun.*, **30**, 265 (1979).
7. Hardouin, F. and Levelut, A. M., *J. Phys.*, **41**, 41 (1980).
8. Levelut, A. M., Tarento, R. J. et al., *Phys. Rev.*, **A24**, 2180 (1981).
9. Sigaud, G., Hardouin, F. et al., *J. Phys.*, **40**, C3-356 (1979).
10. Hardouin, F., Levelut, A. M. et al., *Solid State Commun.*, **33**, 337 (1980).
11. Hardouin, F., Levelut, A. M. et al., *J. Phys.*, **42**, 71 (1981).
12. Prost, J., *J. Phys.*, **40**, 581 (1979).
13. Longa, L. and de Jeu, W. H., *Phys. Rev.*, **A28**, 2380 (1983).

14. McMillan, W. L., *Phys. Rev.*, **A4**, 1238 (1971).
15. Benguigui, L. and Hardouin, F., *J. Phys. Lett.*, **42**, 1381 (1981).
16. Meyer, R. B. and Lubensky, T. C., *Phys. Rev.*, **A14**, 2307 (1976).
17. McMillan, W. L., *Phys. Rev.*, **A6**, 936 (1972).
18. Landau, L. D. and Lifshitz E. M., "*Electrodynamica sploshnykh sred*" (M. Nauka, 1982).